

10/529366

Figure 1. Triglyceride content of a *Drosophila* CG7042 (GadFly Accession Number CG7042-PA) mutant

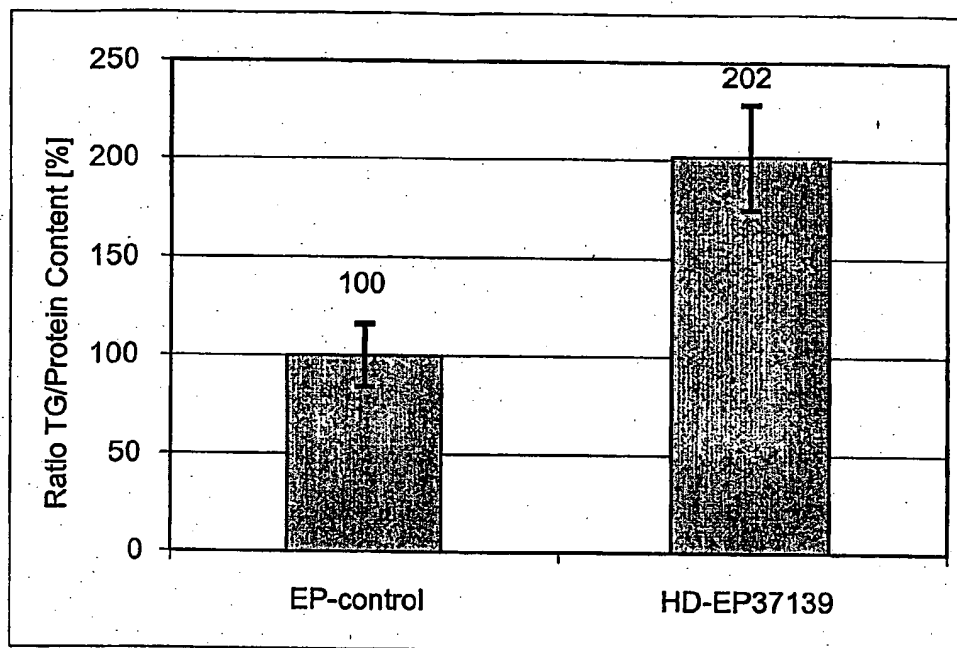
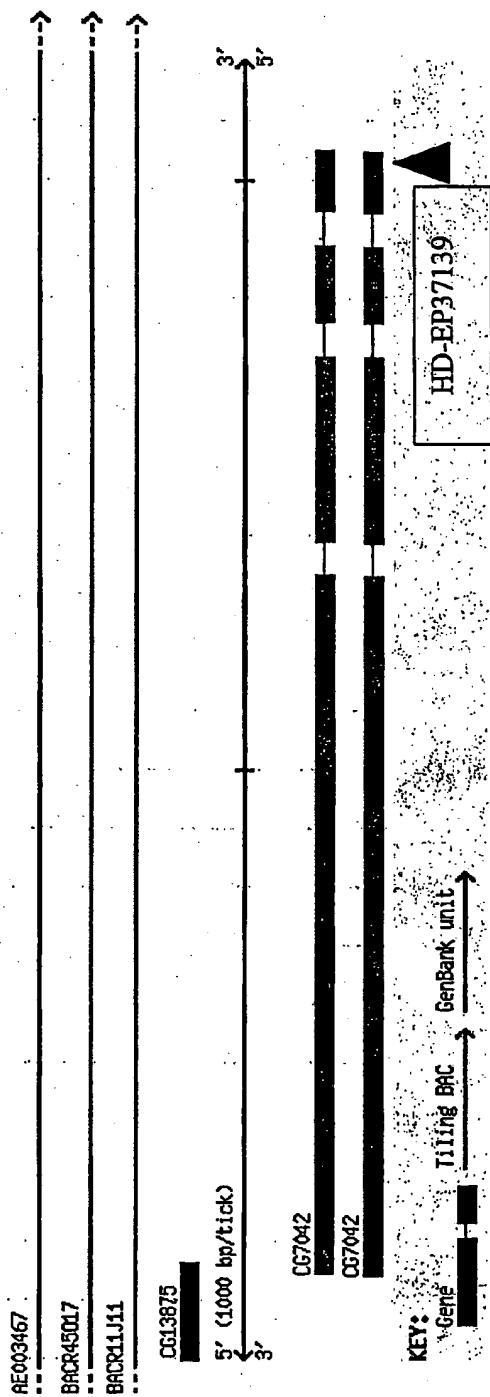


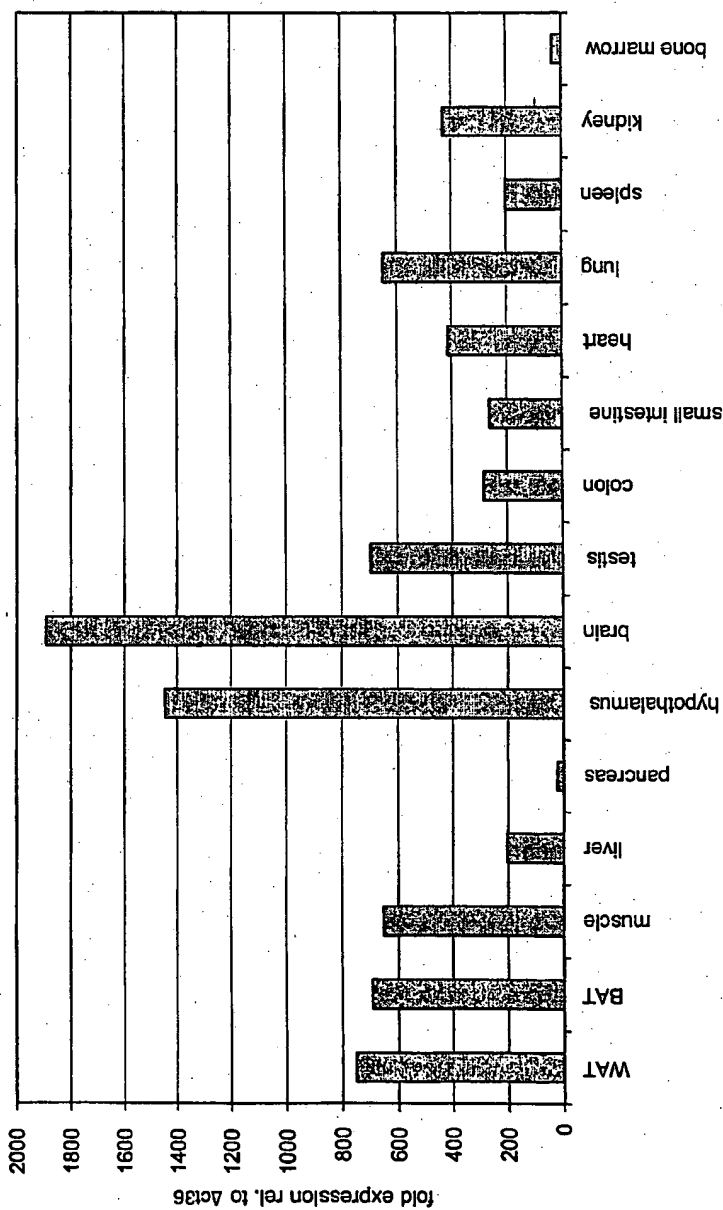
Figure 2. Molecular organization of the CG7042 gene (GadFly Accession Number CG7042-PA)



10/529366

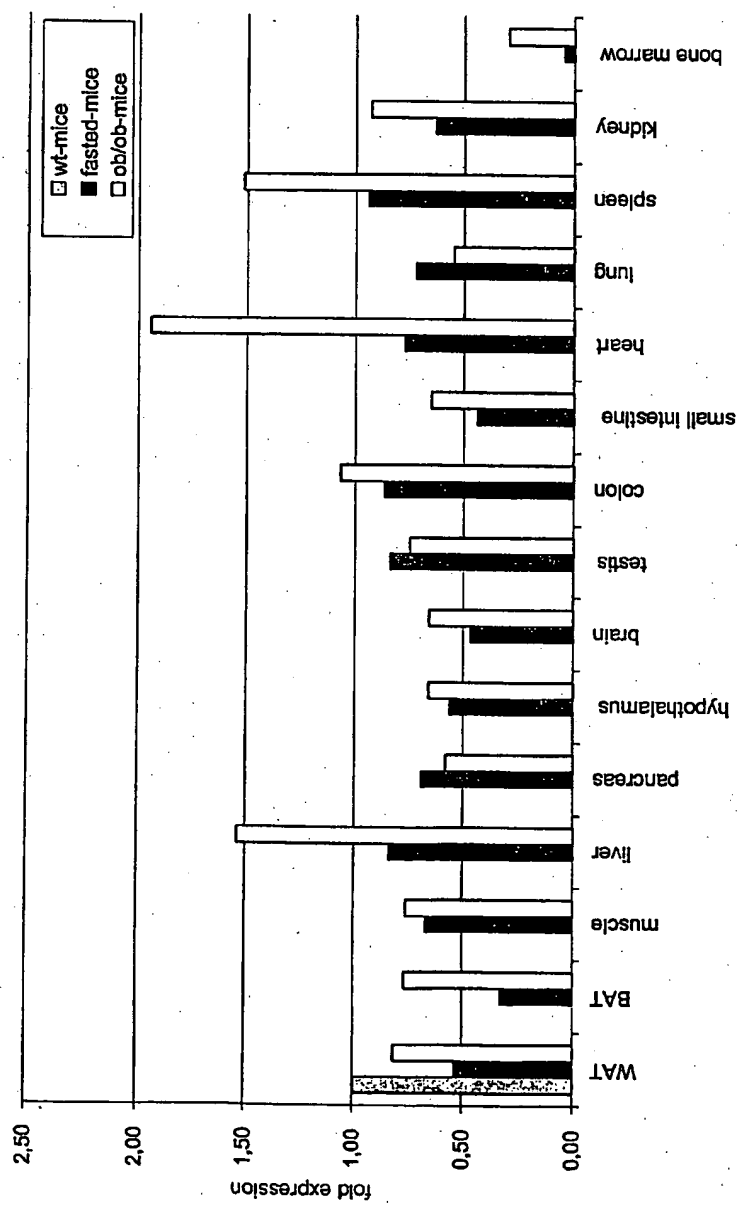
Figure 3. Expression of the CG7042 (GadFly Accession Number) Homolog in Mammalian Tissues

Figure 3A. Real-time PCR analysis of protein similar to DUAL-SPECIFICITY PHOSPHATASE TS-DSP1 (TS-DSP1) expression in wild type mouse tissues



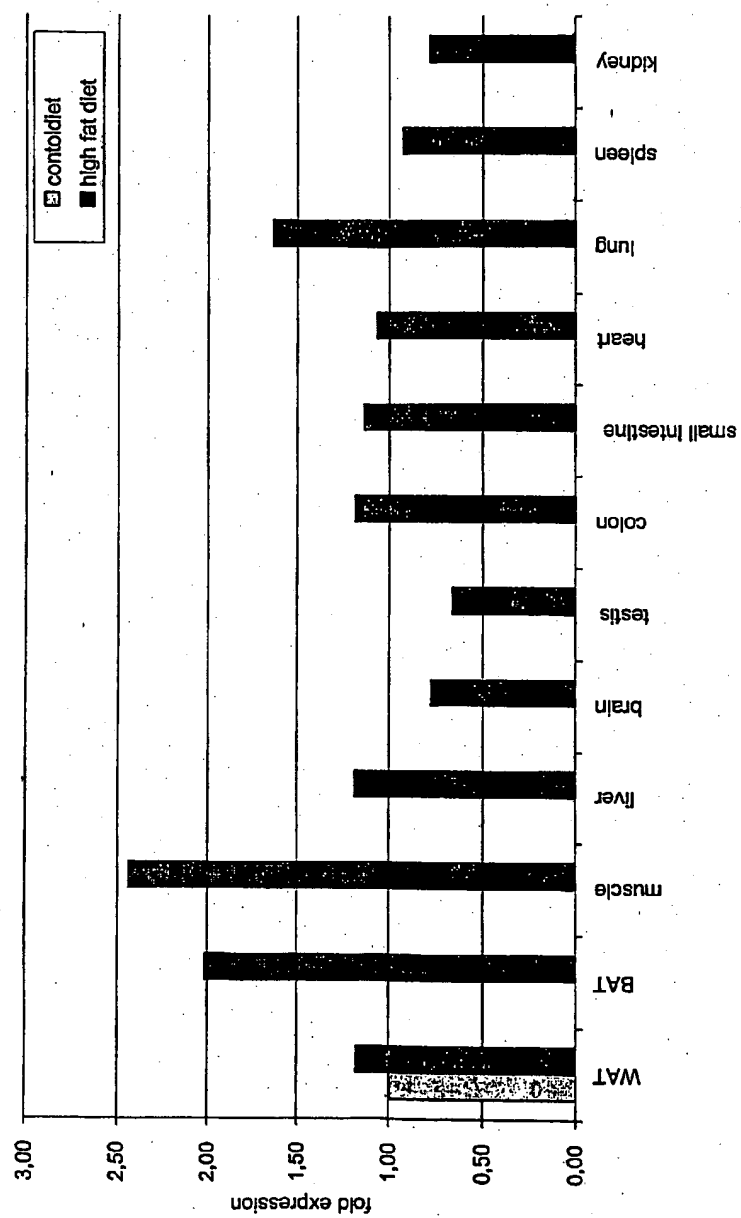
10/529366

Figure 3B. Real-time PCR analysis of TS-DSP1 expression in different mouse models



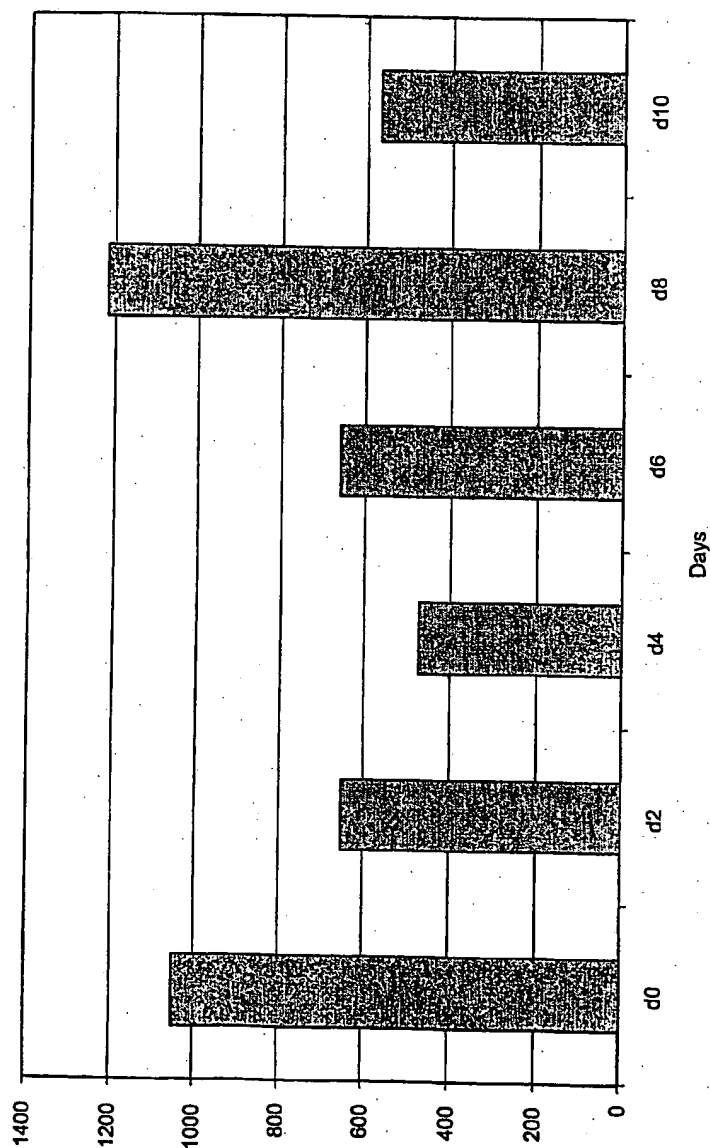
10/529366

Figure 3C. Real-time PCR analysis of TS-DSP1 expression in mice fed with a high fat diet compared to mice fed with a control diet



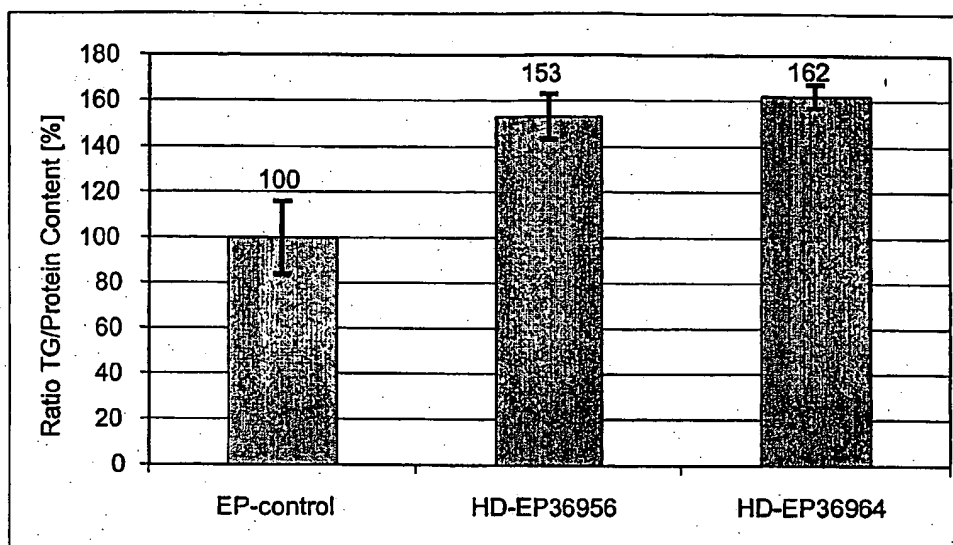
10/529366

Figure 3D. Real-time PCR analysis of TS-DSP1 expression in 3T3-L1 cells differentiated from preadipocytes to mature adipocytes



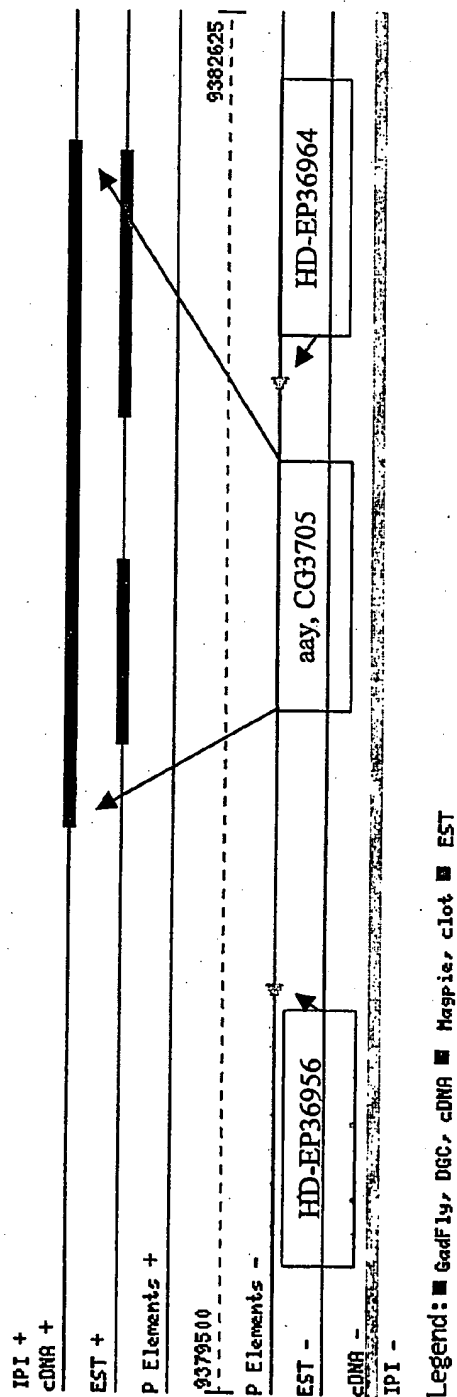
10/529366

Figure 4. Triglyceride content of a *Drosophila astray* (GadFly Accession Number CG3705) mutant



10/529366

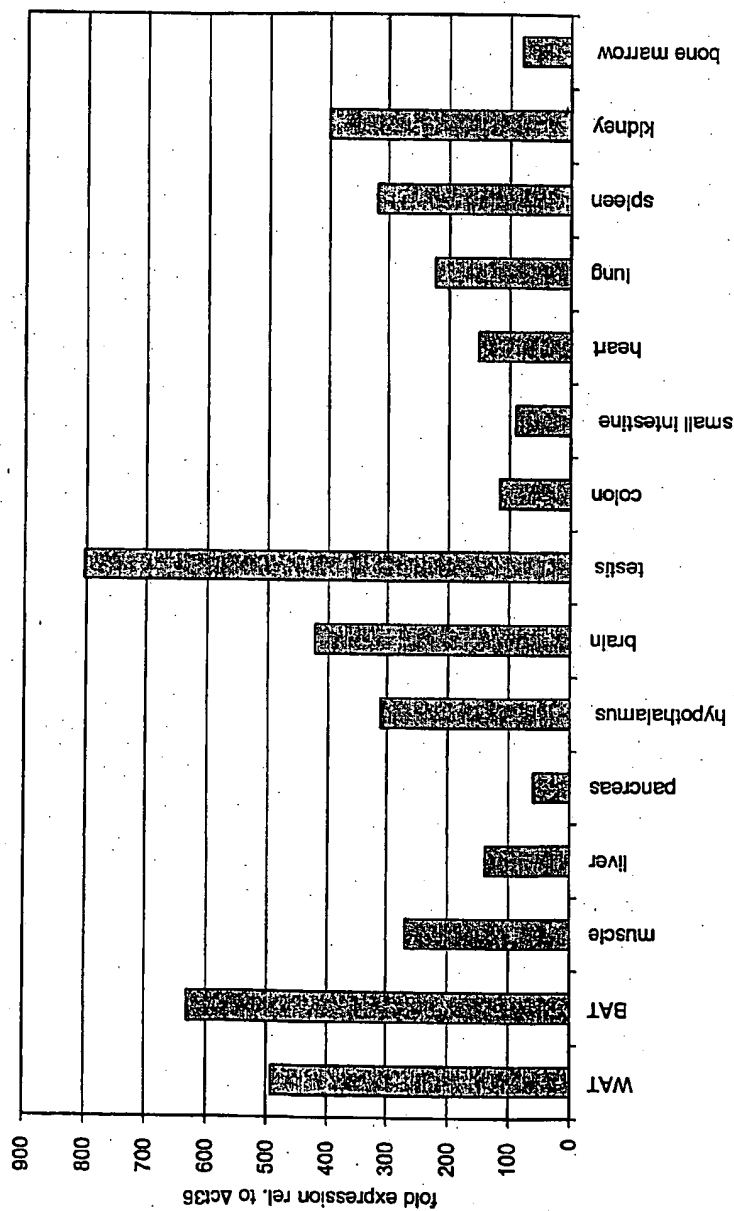
Figure 5. Molecular organization of the *asray* gene (*aay*; GadFly Accession Number CG3705)



10/529366

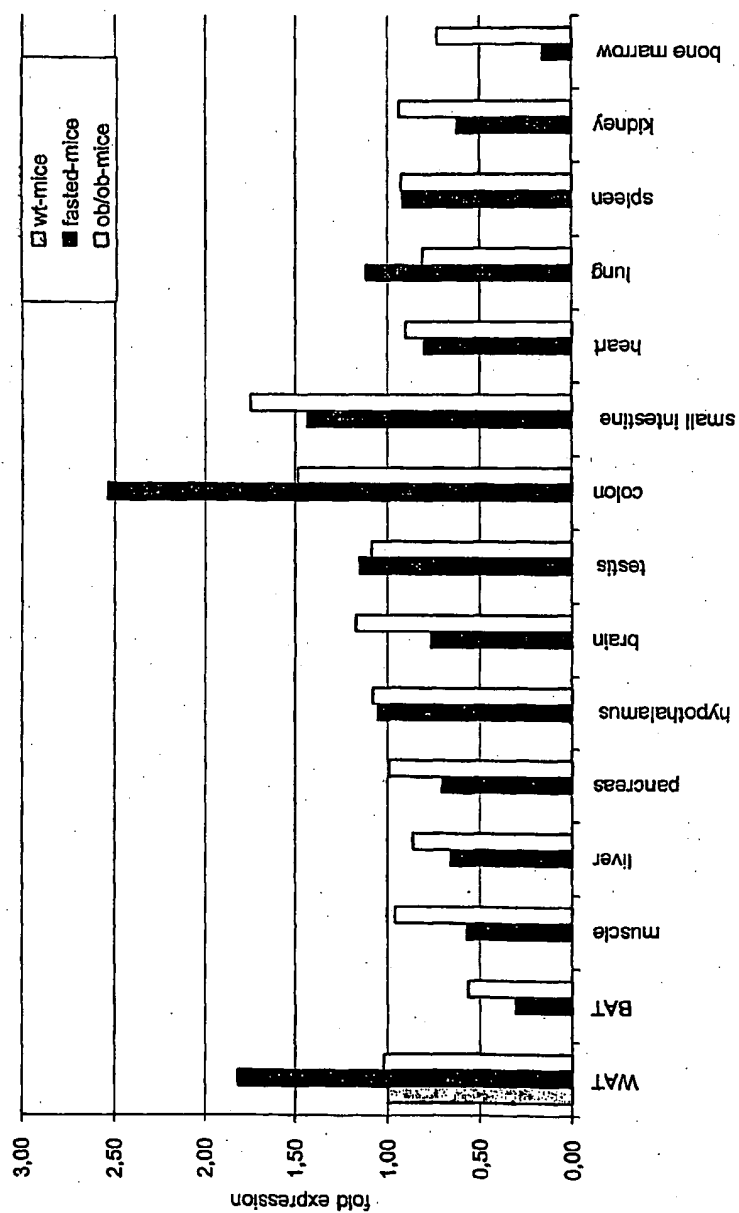
Figure 6. Expression of the *astray* Homolog in Mammalian Tissues

Figure 6A. Real-time PCR analysis of phosphoserine phosphatase (Psph) expression in wild type mouse tissues



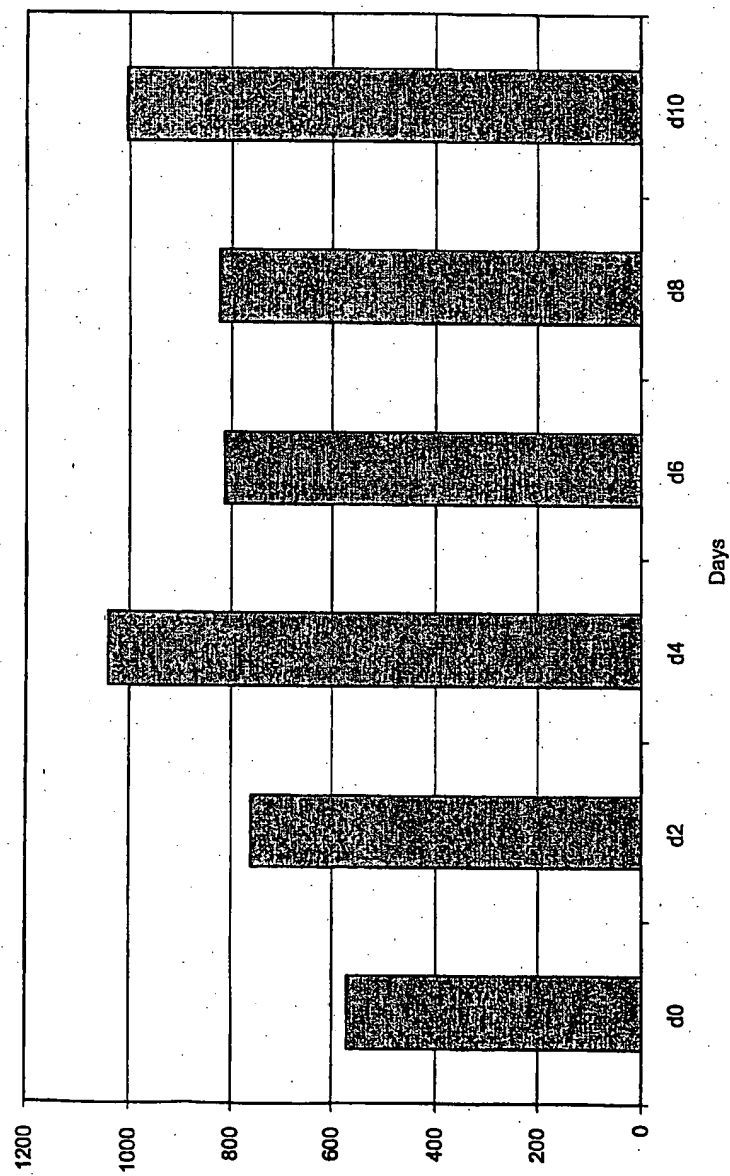
10/529366

Figure 6B. Real-time PCR analysis of PspH expression in different mouse models



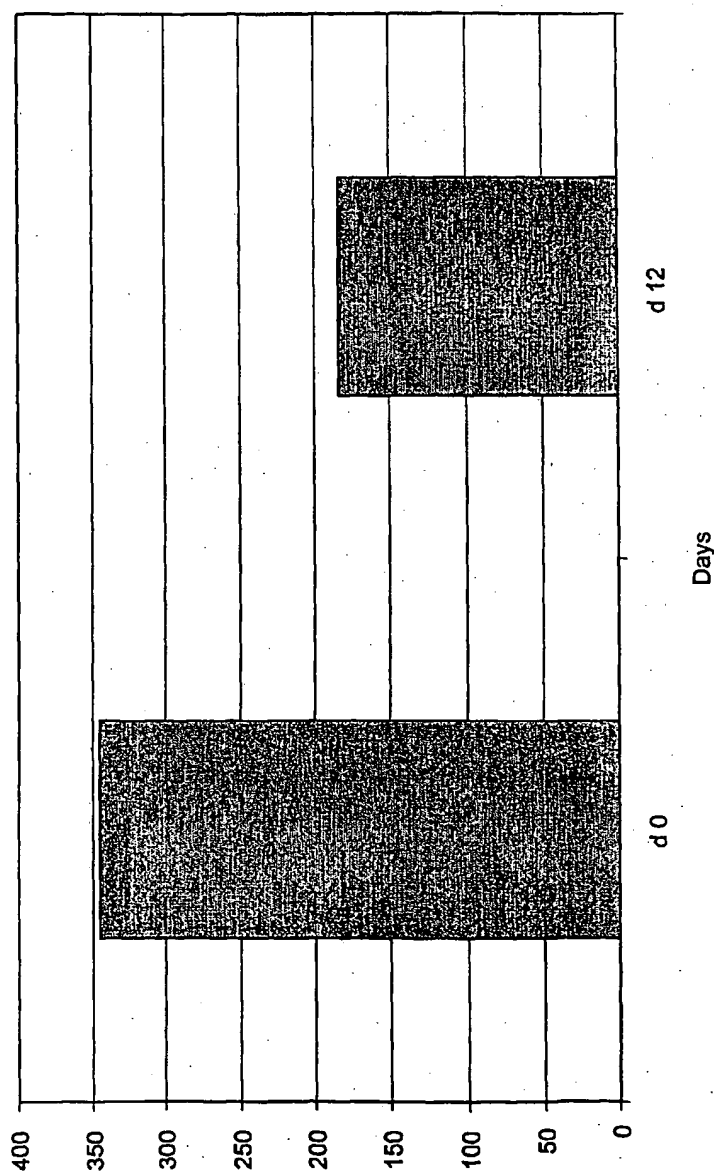
10/529366

Figure 6C. Real-time PCR analysis of PspH expression in 3T3-L1 cells differentiated from preadipocytes to mature adipocytes



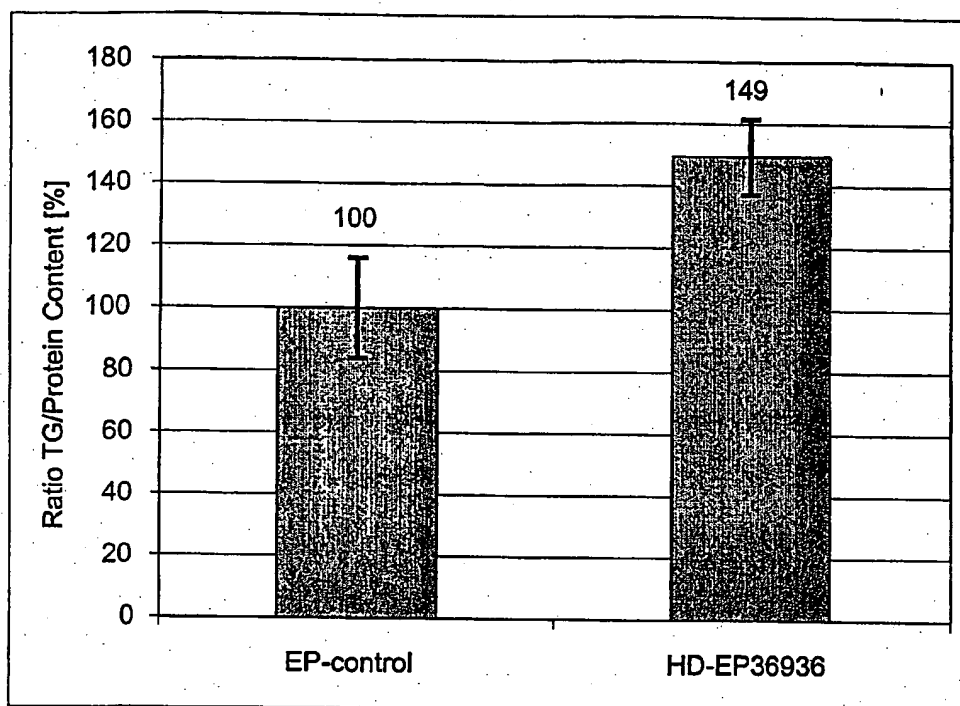
10/529366

Figure 7. Expression of the human *astray* homolog in mammalian (human) tissue. Microarray analysis of phosphoserine phosphatase (PSPH) expression in human adipocyte cells during the differentiation from preadipocytes to mature adipocytes

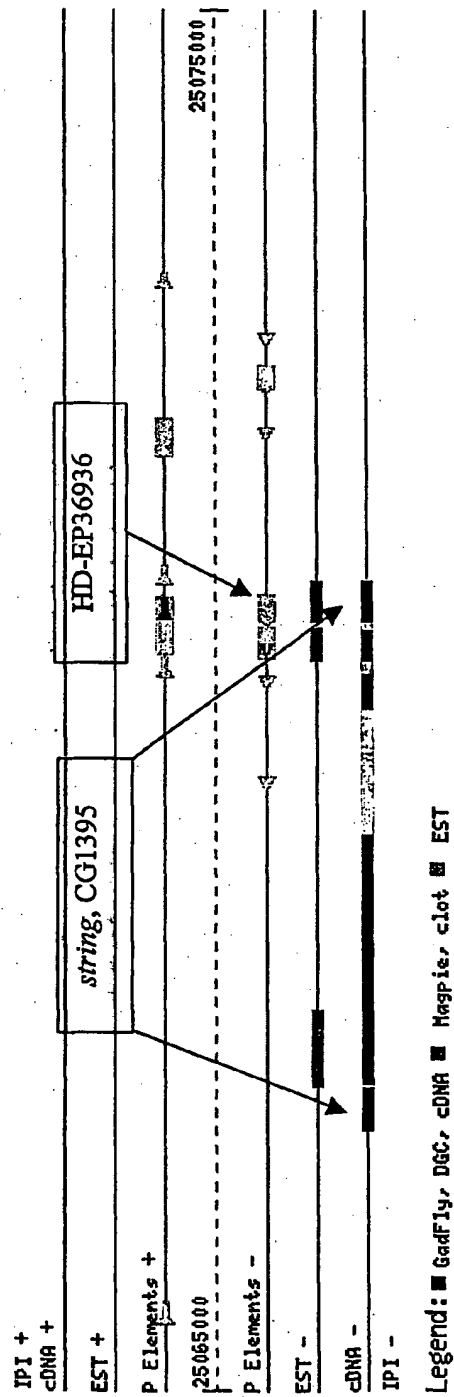


10/529366

Figure 8. Triglyceride content of a *Drosophila string* (GadFly Accession Number CG1395) mutant

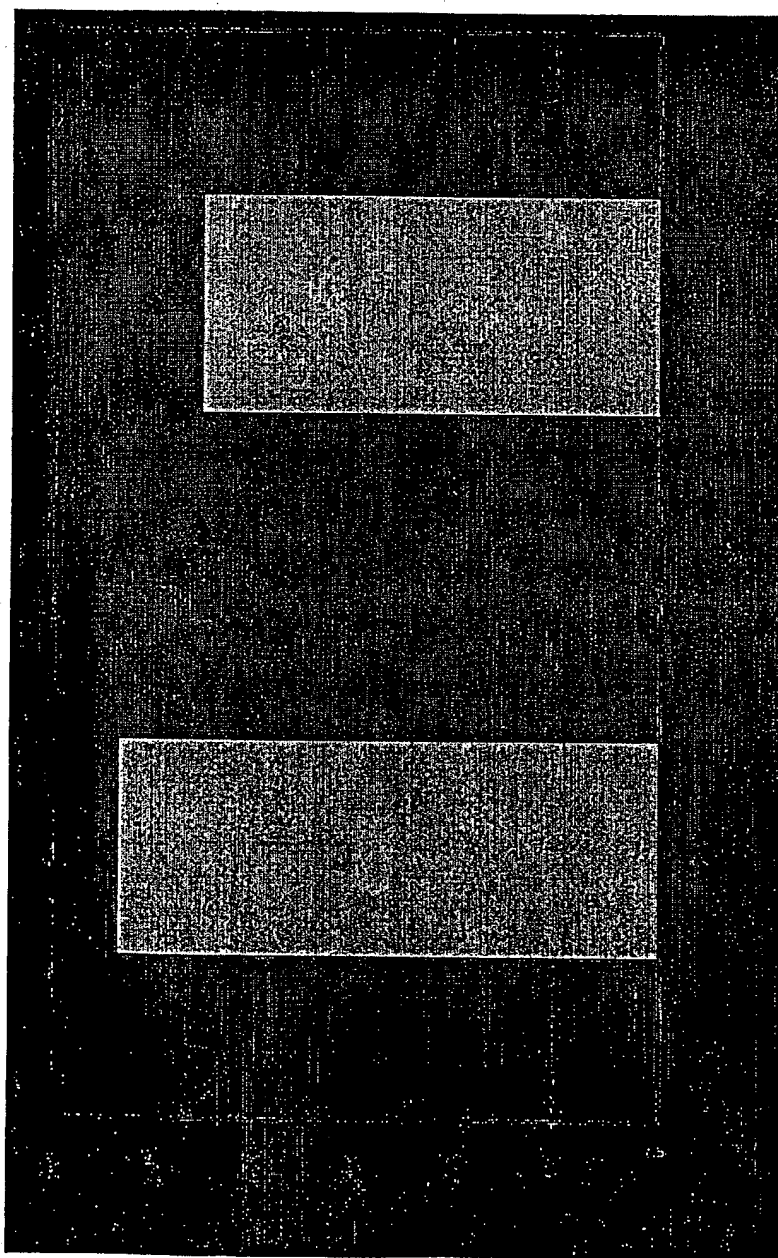


10/529366

Figure 9. Molecular organization of the *string* gene (GadFly Accession Number CG1395)

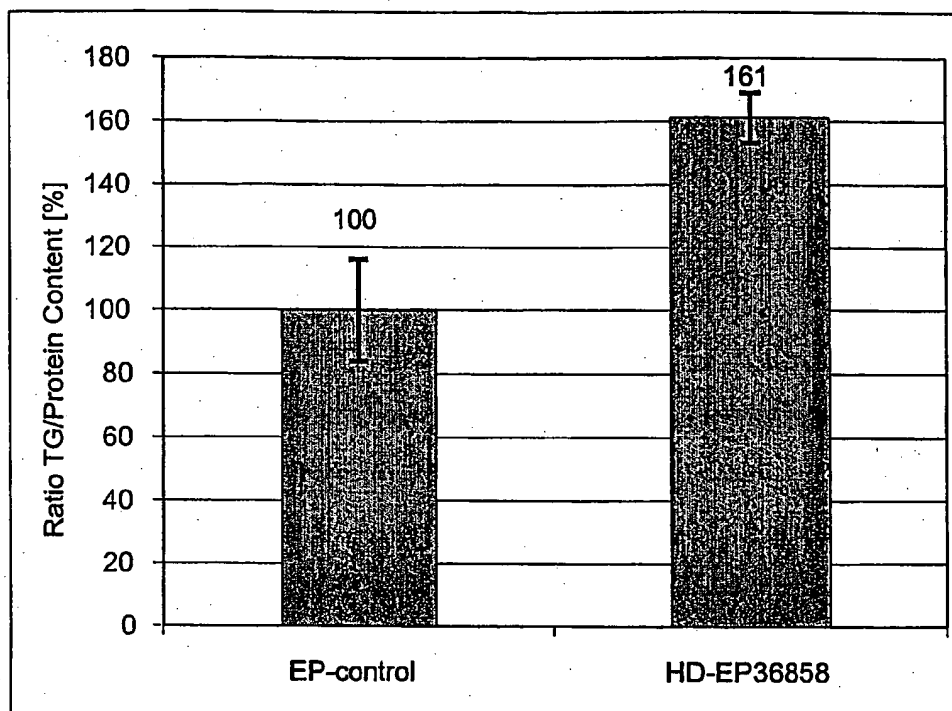
10/529366

Figure 10. Expression of a human *string* homolog in mammalian (human) tissue. Microarray analysis of cell division cycle 25B (CDC25B) expression in human adipocyte cells during the differentiation from preadipocytes to mature adipocytes



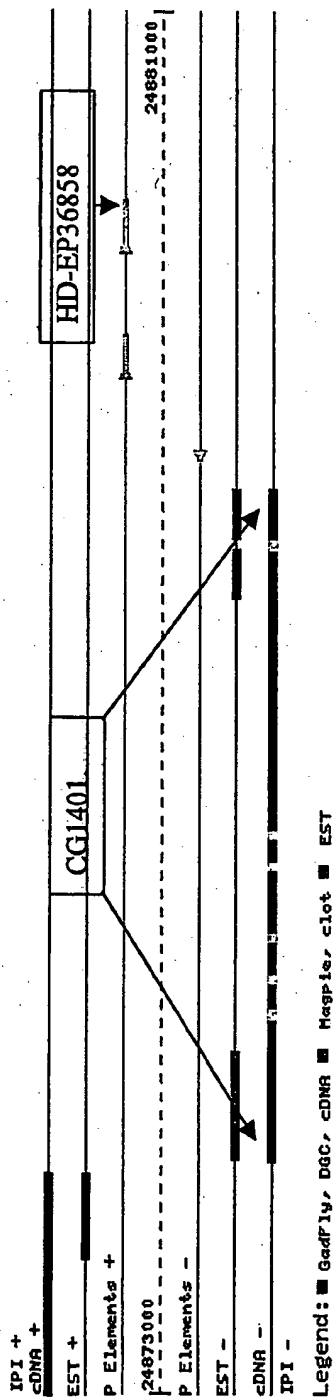
10/529366

Figure 11. Triglyceride content of a *Drosophila* CG1401 (GadFly Accession Number) mutant



10/529366

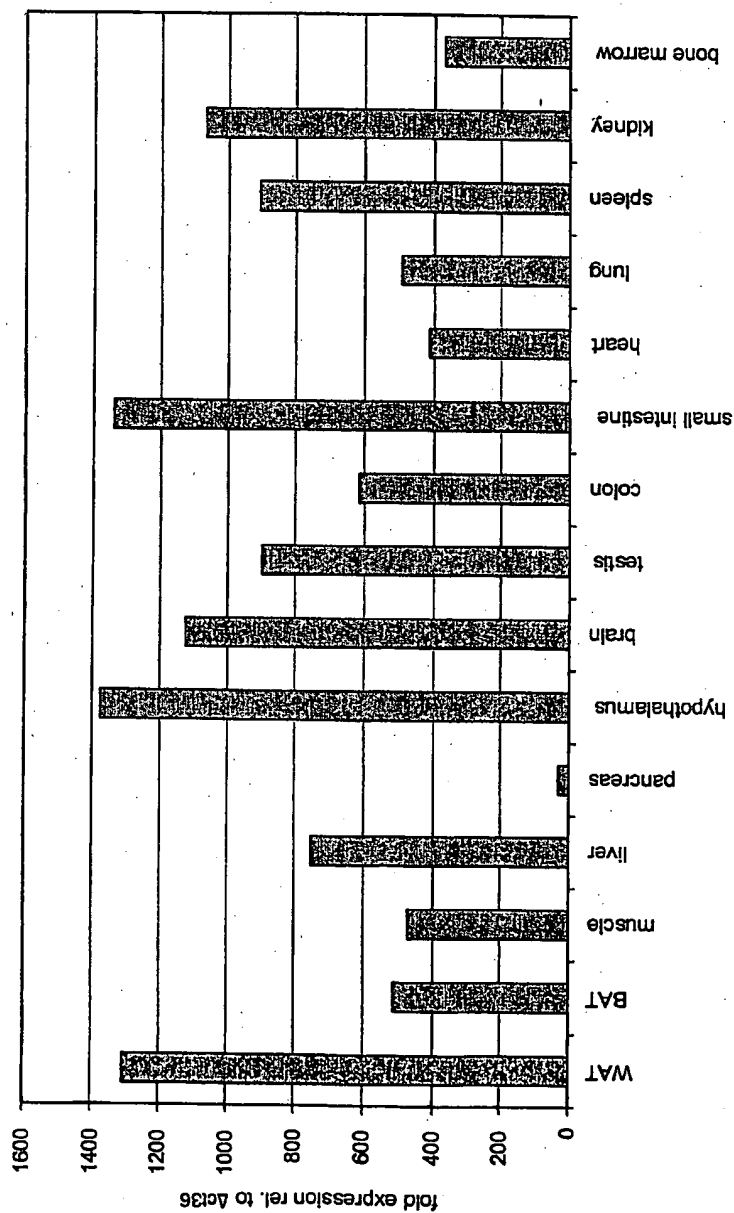
Figure 12. Molecular organization of the CG1401 gene (GadFly Accession Number)



10/529366

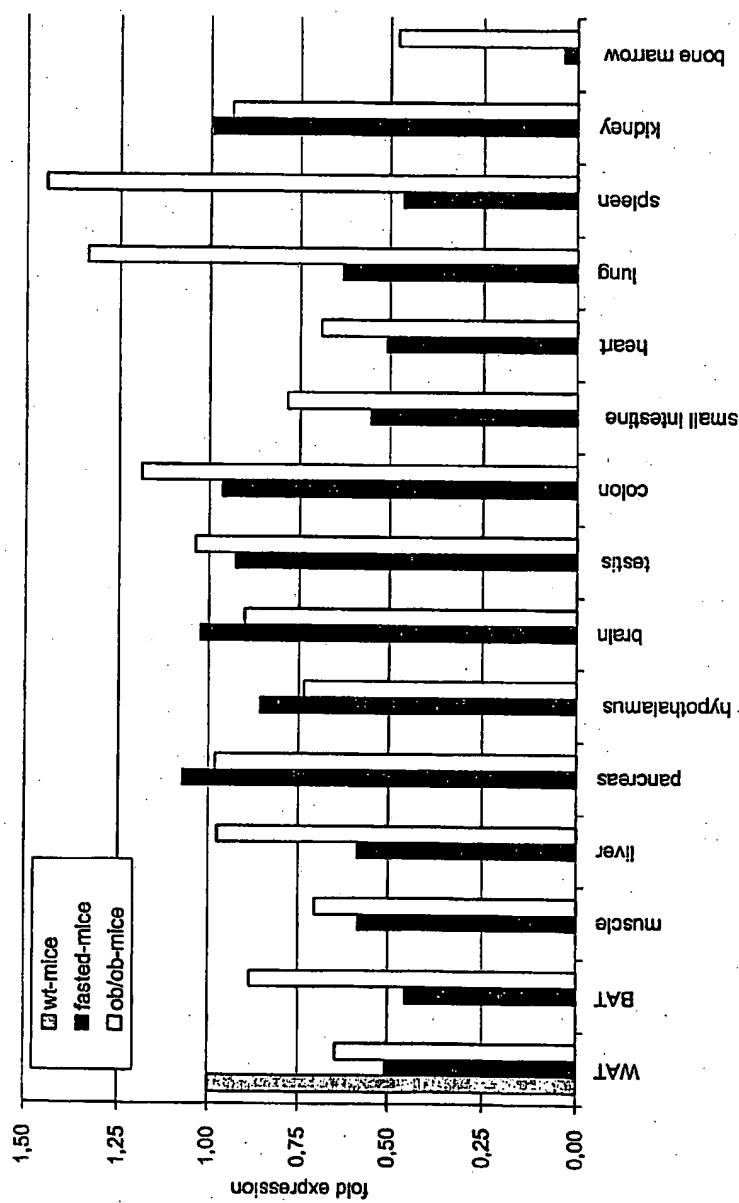
Figure 13. Expression of CG1401 (GadFly Accession Number) Homologs in Mammalian Tissues

Figure 13A. Real-time PCR analysis of RIKEN cDNA 4921514I20 gene (4921514I20Rik) expression in wild type mouse tissues



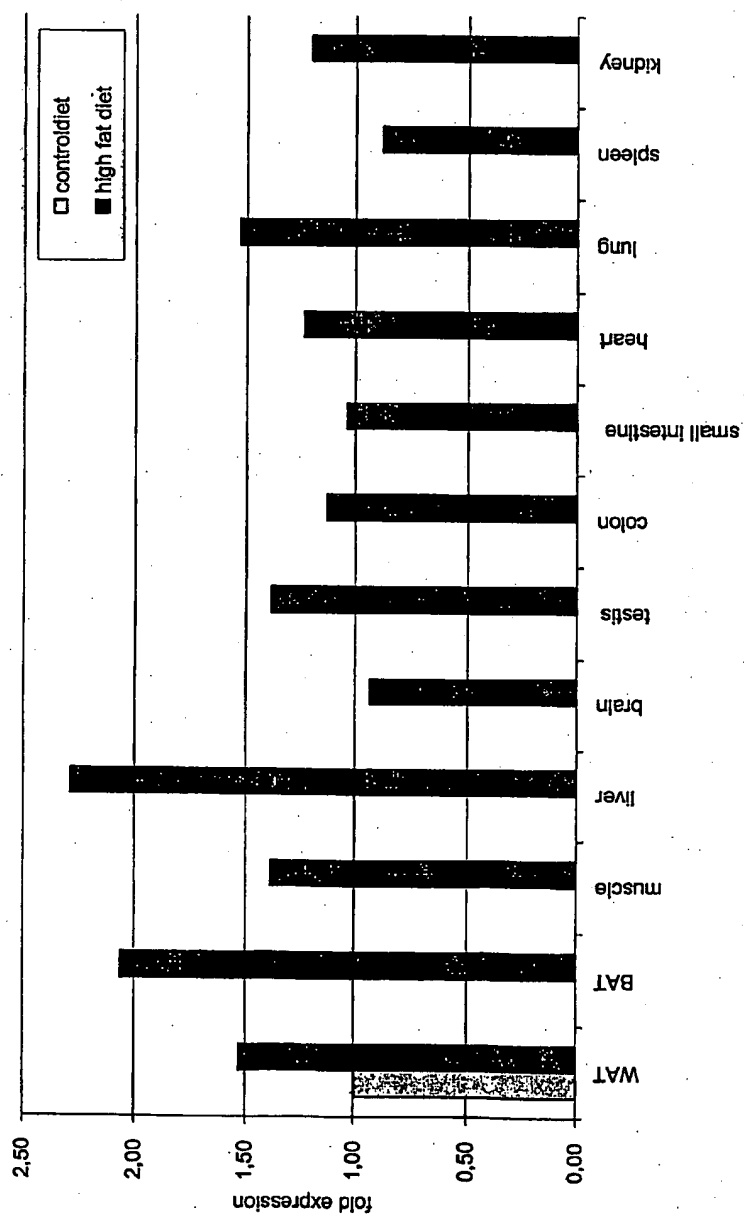
10/529366

Figure 13B. Real-time PCR analysis of 4921514T20Rik expression in different mouse models



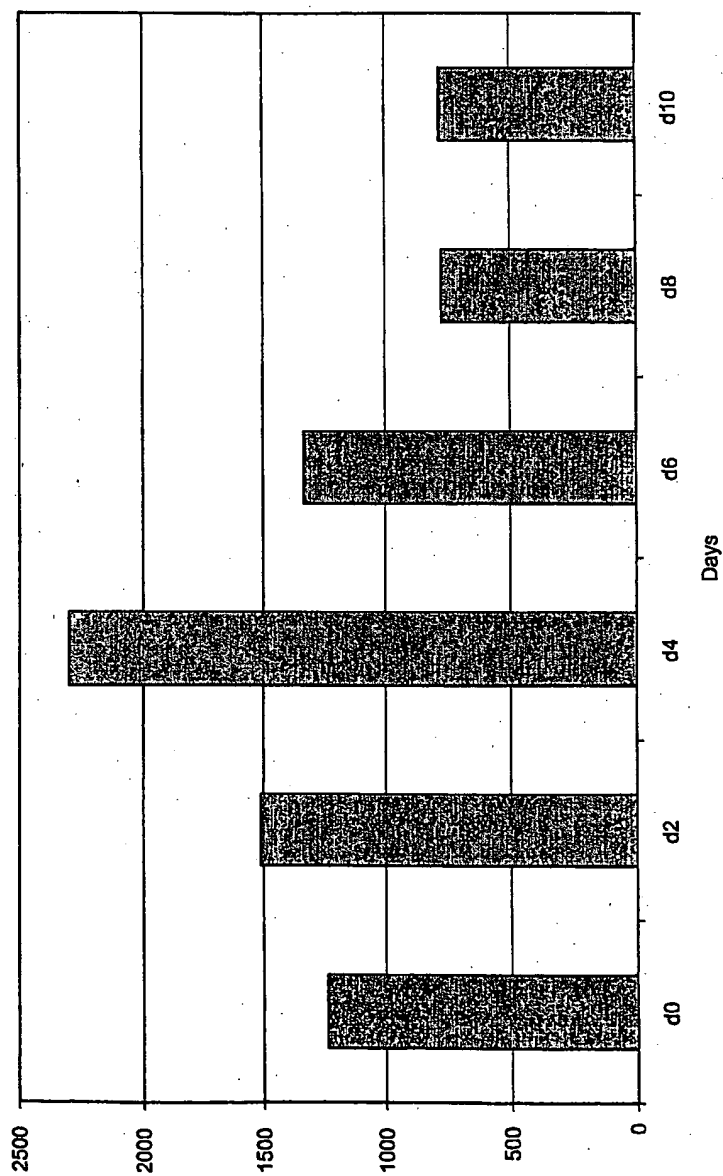
10/529366

Figure 13C. Real-time PCR analysis of 4921514I20Rik expression in mice fed with a high fat diet compared to mice fed with a control diet



10/529366

Figure 13D. Real-time PCR analysis of 4921514I20RIk expression in 3T3-L1 cells differentiated from preadipocytes to mature adipocytes



10/529366

Figure 14. Expression of the human CG1401 homolog in mammalian (human) tissue. Microarray analysis of cullin 5 (CUL5) expression in human adipocyte cells during the differentiation from preadipocytes to mature adipocytes

